Transport in Porous Media **3** (1988), 17–34

Fluid Topology, Pore Size and Aspect Ratio During Imbibition

NORMAN C. WARDLAW
Department of Geology and Geophysics, University of Calgary, Calgary, Alberta T2N 1N4, Canada

and

LI YU
Nanhai West Oil Corporation, PO Box 11, Potou, Zhanjiang, Guangdong, People's Republic of China

(Received: 23 January 1987; revised: 18 November 1987)

Abstract. Imbibition in glass micromodels for air-mercury and water-oil systems occurs by wetting phase (wp) cluster growth and frontal drive processes. Lower capillary number and higher wetting phase (wp) saturation at the start of imbibition favour cluster growth.

Imbibition experiments for both fluid systems show that the 'rules' of nwp withdrawal are related to pore size and to fluid topology as well as to aspect ratio. The emptying of a pore is favoured by small size, small aspect ratio (size 'rules'), and fewer connected throats occupied by nonwetting phase (nwp) (fluid topology 'rules').

The relative importance of fluid topology compared with pore size in determining the sequence of nwp withdrawal from pores is affected by the initial nwp saturation, pore size variability, pore-throat size ratio, pore and throat shape and contact angle. High initial nwp saturation, small variability of pore size and small pore-throat diameter ratio are all factors which increase the effects of fluid topology in determining nwp withdrawal sequence. Under these conditions, nwp displacement efficiency is larger because withdrawal occurs first from 'dead-end' branches without breaking the continuity of the nwp conducting pathways to the nwp sink. The high nwp displacement efficiency obtained in unconsolidated sands may be explained by the importance of topology 'rules' during imbibition in these low aspect ratio media.

Key words. Imbibition, fluid topology, pore size, aspect ratio, cluster growth, frontal drive.

0. Nomenclature

Roman Letters

D	effective diameter of pore or throat given by $2 \div F(\epsilon)(1/x + 1/y)$, m
$F(\epsilon)$	nondimensional term which varies as a function of cross-sectional shape (Lenormand *et al.*, 1983)
L	external dimension of the network (width or length), m
N_{ca}	capillary number in the network, dimensionless
nwp	nonwetting phase
P	any capillary pressure, Pa
P_{I1}	capillary pressure for nwp to withdraw from a pore which has one connected throat occupied by nwp, Pa

P_{I2} capillary pressure for nwp to withdraw from a pore which has two adjacent connected throats occupied by nwp, Pa
Q total volume flow rate in the network, m^3/s
S_{wi} percent of pore volume occupied by wp at the end of drainage and start of imbibition, dimensionless
S_{ni} percent of pore volume occupied by nwp at the end of drainage and start of imbibition, i.e. $100 - S_{wi}$, dimensionless
S_{nr} percent of pore volume occupied by trapped nwp at the end of imbibition, dimensionless
v velocity, m/s
wp wetting phase
X_I diameter of $I2$ interface in plan, m
X_P diameter of pore in plan, m
X_T width of throat, m
Y_P depth of pore, m
Y_T depth of throat, m
Z number of throats connected to each pore (coordination number)

Greek Letters

γ interfacial tension, N/m
θ contact angle, degrees
μ viscosity, Pa · s

1. Introduction

Drainage capillary pressures are related to the curvatures of interfaces in constrictions (throats) within pore systems, whereas imbibition capillary pressures are related to the curvatures of interfaces in bulges (pores). Interface curvatures within pores are affected by the positions of directly connected throats occupied by nonwetting phase (fluid topology) as well as by the sizes and shapes of these throats. These factors complicate the interpretation of pore size from capillary pressure curves. The degree of irregularity of advancing fluid fronts and the efficiency with which one fluid displaces another vary in response to the effects of pore size and fluid topology. A major objective of this presentation is to provide a better understanding of interface movements and their effects on the displacement of one fluid by another during imbibition. Experiments were performed in two-dimensional glass micromodels for air-mercury and for water-oil (water-wet) systems.

For piston-type movement of interfaces where only one connected throat is occupied by nwp, the relationship between capillary pressure and pore size is given by the Young–Laplace equation:

$$P_c = 4\gamma \cos\theta / D, \tag{1}$$

where γ is surface tension, θ is contact angle, and D is the effective diameter of the pore.

However, as shown by Lenormand *et al.* (1983, Table 1), the withdrawal of an interface at a junction point of four ducts occurs at successively lower pressures depending on whether one, two or three of the ducts (throats) are occupied by nwp. Thus, the number and arrangement of throats occupied by nwp affects the withdrawal pressure.

The models used in this study differ from those of Lenormand *et al.* (1983) in having pores (bulges) as well as throats (constrictions), but we adopt their terminology. Withdrawal of nwp from a pore with nwp in one throat is referred to as imbibition of type $I1$, withdrawal with two adjacent throats occupied by nwp is $I2$ and other configurations $I2A$, $I3$, and $I4$ are as shown in Figure 1. The emptying of a pore is favoured by small size, small aspect ratio, and fewer connected throats occupied by nwp.

The relative importance of fluid topology compared with pore size in determining the sequence of nwp withdrawal from pores is affected by the initial nwp saturation, pore size variability, pore-throat size ratio, pore and throat shape, and contact angle. High initial nwp saturation, small variability of pore size, and small pore-throat diameter ratio all are factors which increase the effects of fluid topology in determining nwp withdrawal sequence. Under these conditions, nwp displacement efficiency is larger because withdrawal occurs first from 'dead-end' branches without breaking the continuity of the nwp conducting pathways to the nwp sink.

Other types of interface motion involving saddle-shaped (anticlastic) menisci can occur within pores as well as throats (Li and Wardlaw, 1986b) but are rare in the experiments reported here because of the relatively small pore size to throat size ratio in the model used.

Although motions of individual interfaces obey the above 'rules', fluid advance during imbibition can be by frontal drive, cluster growth or by a combination of these processes. The type of advance is affected by initial nwp topology, capillary number and pore geometry.

In frontal drive, wp displaces nwp at a linear (two dimensions) advancing front (Figure 2A). In the case of cluster growth, discontinuous region (finite domains)

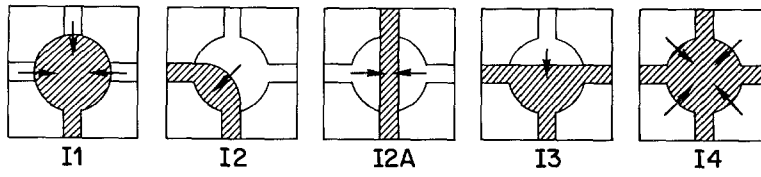

Fig. 1. Pore connected by four throats illustrates fluid topology of five types. Shaded areas are nwp and other areas wp.

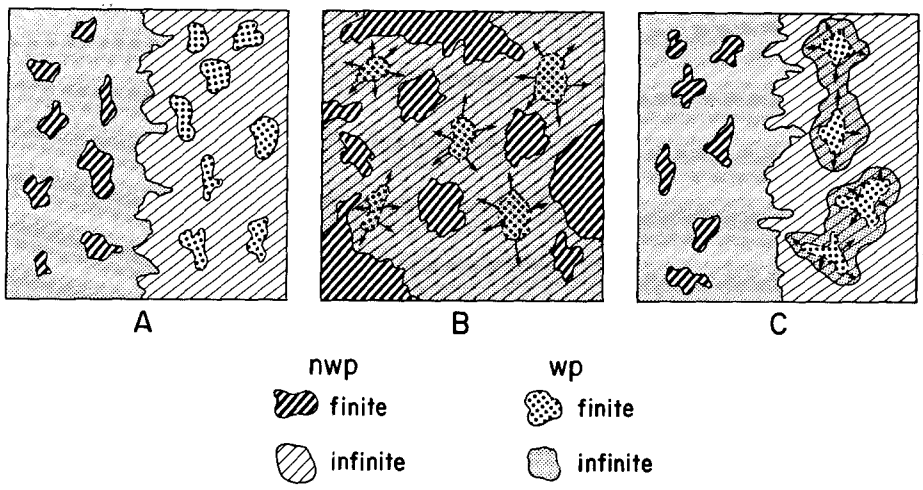

Fig. 2. Imbibition by (A) frontal advance (wetting phase advances from left to right); (B) cluster growth; and (C) combination of frontal advance and cluster growth. In B and C, the finite domains of wp enlarge in all directions by cluster growth (arrows) to form infinite wp domains. These changes are indicated by overlaying the symbols for infinite nwp (initial condition) and infinite wp (final condition) in the regions where nwp is displaced by wp.

of wp enlarge and eventually intersect to form continuous regions (infinite domains) and, in the process, trap nwp.

Cluster growth requires that wetting phase has continuity as wetting films covering the rough surfaces of pore walls or occupying small spaces at edges and corners of pores. Domains of wp which appear macroscopically discontinuous are able to enlarge by addition of wp which is transported along surface films and along edges and corners occupied by wp. Wetting phase transport in such situations has been referred to in several papers (Morrow, 1971; Dullien *et al.*, 1986; Lenormand and Zarcone, 1984a, b; Takamura, 1982; Mason and Morrow, 1984; Chen, 1986; Mohanty *et al.*, 1980, 1981; Mohanty and Salter, 1982; Mahers and Dawe, 1985).

Lenormand and Zarcone (1984a) and Chatzis and Dullien (1981) have illustrated frontal drive in two-dimensional micromodels. Lenormand and Zarcone (1984a) also report a type of cluster growth, referred to as nucleation cluster growth (1984a, b) in which the porous structure is initially 100% filled with nwp and wp 'seeds' nucleated by local snap-off events. They provided theory and observations that capillary number ($N_{ca} = Q\mu/LY\gamma$) affects the type of displacement process (1984a). At low capillary numbers ($N_{ca} < 10^{-6}$), wp flow along roughness is important and cluster growth occurs. At higher capillary numbers ($N_{ca} > 10^{-4}$), wp flows in the bulk spaces of ducts (pores) and the mechanism is frontal drive.

Experiments reported in this paper show that at constant N_{ca}, the extent to which frontal drive or cluster growth occurs also is affected by the nwp saturation at the start of imbibition. Higher initial nwp saturation favours frontal drive.

2. Materials and Methods

Glass micromodels were made using the method described by McKellar and Wardlaw (1982). Mirror image patterns were etched with hydrofluoric acid on two glass plates which were then registered and sealed at the lateral edges. A nwp source duct connects with a moat along one edge of the model. The opposite edge of the model is separated from a wp sink moat and duct by the space separating the two glass plates. This space is ~ 20 μm and, since this is smaller than the smallest throat, it acts as a capillary barrier. The model can be completely filled with nwp without nwp passing the barrier into the wp sink.

The model consists of a square lattice of 80 sites (pores) on a side with four bonds (throats) connecting with each pore. The model is 8 cm^2. The centers of the pores are equidistant and the pores are circular in outline. All throats are smaller than pores and there are five sizes of each. Pores and throats both have uniform size distributions, i.e., there are equal numbers of pores in each of the five different size categories and the same is true for the five size categories of throats. Pores and throats of different sizes are randomly arranged with respect to each other. The original image of the model was computer drafted and photo-reduced. This model is referred to as an uncorrelated pore-throat (UPT) model.

The average cross-sectional shapes of throats and pores is shown in Figure 3. The effective diameters of pores and throats were obtained from measurements of their widths (x) and depths (y) (Figure 4). The effective diameter (D) is given by (Lenormand *et al.*, 1983):

$$D = \frac{2}{F(\epsilon)\left(\frac{1}{x} + \frac{1}{y}\right)} \tag{2}$$

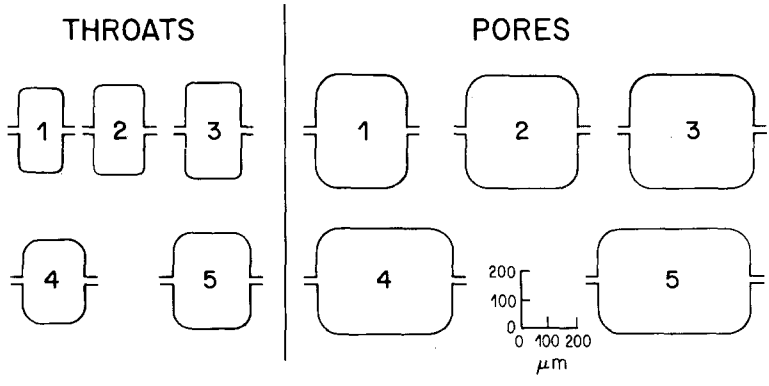

Fig. 3. Cross-sectional shapes of throats and pores drawn to scale. These sections do not illustrate small scale surface roughness which is also present.

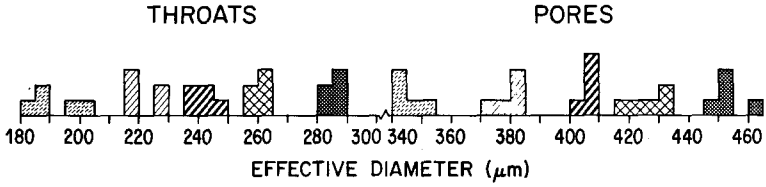

Fig. 4. Effective diameters (D) for throats and pores of five different sizes.

and, for $x \gg y$:

$$D \cong 2y \tag{3}$$

$F(\epsilon)$ is a nondimensional term which varies as a function of cross-sectional shape.

Experiments were conducted with two fluid pairs: air-mercury and water-oil. Air and water were the wetting liquids in each pair. Air is a compressible wp and water an incompressible wp. Although water is incompressible and may appear to be discontinuous at the end point of drainage (S_{wi}), in fact it may have continuity as thin films or filling surface roughness on pores and throats (Dullien *et al.*, 1986).

In air-mercury experiments, pressure on the mercury was increased gradually and the evacuated model filled to an initial saturation over a period of approximately 1 h. The initial nwp saturation ($S_{ni} = 100 - S_{wi}$) at the start of nwp withdrawal was varied in successive experiments from ~92% to 100% (Table I). Mercury was withdrawn by lowering pressure and volume was measured by adjusting the mercury level to a marker on the sight glass and taking a volume reading from the Ruska pump. The time for withdrawal was ~1.5 h. Air advancing contact angles were ~45° and air-mercury interfacial tensions ~480 mN/m.

The fluids in the water-oil experiments were glycerine-water solutions (68 mPa · s viscosity at 22°C) and light paraffin oil (46 mPa · s viscosity at 22°C). Water advancing contact angles were ~30° and interfacial tensions ~20 mN/m. The model was 100% saturated with glycerine-water solution (hereafter referred to as water) and oil was advanced to fill the moat at the nwp source boundary in a manner similar to the air-mercury experiment. The capillary barrier between the model and the wp sink was the same as in the air-mercury experiment and the wp sink was connected to a tube in which water was maintained at a constant elevation during the experiment. Capillary pressure was varied by changing the elevation of the oil level above the horizontal model surface and volume was measured using a burette which could be read with a precision of ±0.01 cc. Drainage proceeded by raising the elevation of the oil and imbibition by lowering it. Duration of drainage was ~1 h and of imbibition ~1.5 h.

Table 1. Experimental observations and results. Imbibition processes are frontal drive and cluster growth. Number % occupancy of pores and throats by nwp at S_{ni} and S_{nr}. Abundance of types of fluid topology at S_{ni} and S_{nr} and preference of pores to be occupied according to size. All data obtained from the same area of the UPT micromodel

Fluids	Imbibition process	% nwp				Fluid topology		Preferences in pore sizes occupied by nwp	
		Pores		Throats					
		S_{ni}	S_{nr}	S_{ni}	S_{nr}	S_{ni}	S_{nr}	S_{ni}	S_{nr}
air-Hg	Frontal	~100	1	~100	0	$I4$ only	$I1$ only		
air-Hg	Frontal + Cluster	96	10	86	4	$I4 > I3 > I2 > I2A > I1$	$I3 > I2A > I1 > I2 > I4$	none	some
air-Hg	Frontal + Cluster	95	11	80	3	$I3 > I4 > I2 > I2A > I1$	$I1 > I2 = I2A > I3 > I4$	none	some
air-Hg	Cluster	93	47	79	22	$I3 > I4 > I2 > I2A > I1$	$I3 > I2A > I4 > I2 > I1$	none	some
air-Hg	Cluster	92	55	77	23	$I3 > I4 > I2 > I2A > I1$	$I3 > I2A > I2 > I1 = I4$	none	some
water-oil	Frontal	87	45	30	15	$I3 > I2 > I1 > I2A > I4$	$I1 > I2 > I3 > I2A > I4$	none	some
water-oil	Frontal	83	40	34	12	$I3 > I2 > I1 > I2A > I4$	$I1 > I2 > I2A > I3 > I4$	none	some

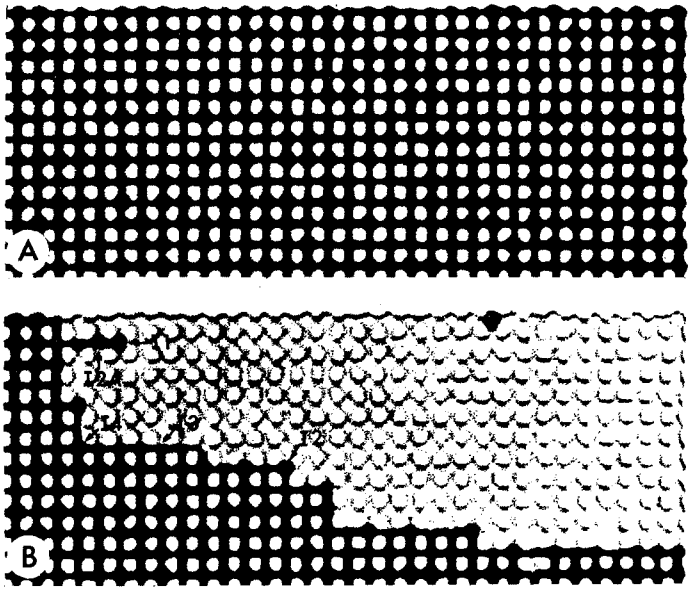

Fig. 5. (A) UPT micromodel 100% saturated with mercury (nwp); (B) mercury withdrawing by frontal advance. Fluid topology of several types is labelled.

3. Results of Air-Mercury Experiments

3.1. FRONTAL DRIVE AND CLUSTER GROWTH

A series of experiments were performed in the same model (UPT), using the same experimental procedures and rates of injection and withdrawal of mercury but with the initial nwp saturation as the only variable.

The model was evacuated and mercury (nwp) advanced until the model was 100% mercury filled. Pressure was lowered and snap-off occurred in a few throats close to the wp (air) source boundary and these provided wp nuclei which enlarged during further decrease of capillary pressure. Frontal drive then proceeded without further snap-off in throats (Figure 5). A regular step-like inter-

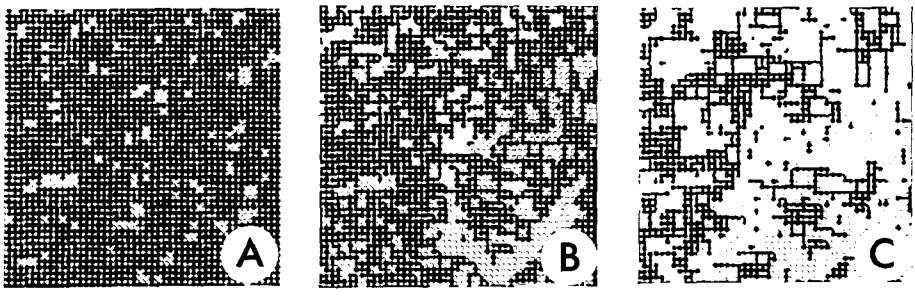

Fig. 6. (A) Initial condition (S_{wi}) with finite wp clusters (air, light coloured) and continuous nwp (mercury, black); (B) cluster growth has commenced, (C) termination of imbibition with discontinuous nwp. Figures illustrate the same portion of the UPT model.

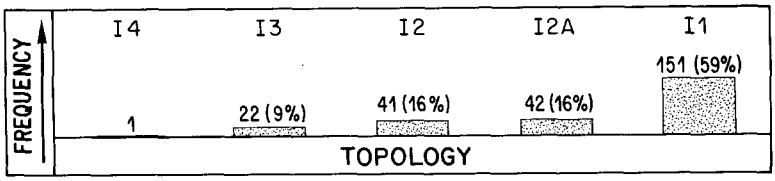

Fig. 7. Fluid topology of pores emptied of nwp (mercury) during mercury withdrawal from an initial condition of 90% mercury saturation in the UPT model.

face advanced without trapping of nwp, except for a few very large pores of greater than critical aspect ratio (Li and Wardlaw, 1986a) where there was local snap-off in throats.

In similar experiments performed from initial nwp saturation of 93%, there was no single front and emptying proceeded by cluster growth (Figure 6). In experiments commenced at 96% nwp a combination of frontal advance and cluster growth was observed (Table I). Higher initial nwp saturations favour frontal drive processes over cluster growth and result in lower residual nwp saturations.

3.2. EFFECTS OF TOPOLOGY AND PORE SIZE DURING IMBIBITION

Mercury was advanced in the UPT model until approximately 90% of the pores were occupied by mercury and mercury was then withdrawn. During withdrawal, a record was made of the topologic type (Figure 1) of each pore from which mercury withdrew (Figure 7).

The frequency of topologic types and the sizes of pores occupied by mercury at the beginning (S_{ni}) and end (S_{nr}) of mercury withdrawal (imbibition) were obtained from photographs of the model. Figure 8 illustrates the frequency of

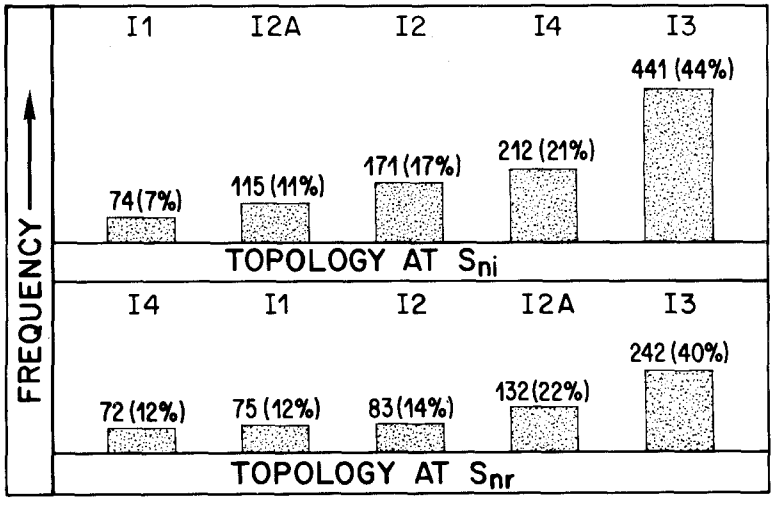

Fig. 8. Fluid topology for pores occupied by nwp at $S_{ni} = 92\%$ and $S_{nr} = 55\%$ for UPT model.

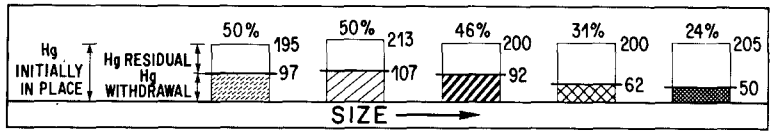

Fig. 9. Illustrates the amount of nwp (mercury) initially in place (S_{ni}), mercury residual (S_{nr}) and mercury withdrawn during imbibition ($S_{ni} - S_{nr}$) for pores of five different sizes. Above each column, mercury withdrawn is shown as a percentage of mercury initially in place. Same system as for Figures 7 and 8.

topologic types at S_{ni} and S_{nr}. Figure 9 illustrates the sizes of pores occupied by mercury at S_{ni} and S_{nr}.

These results show a decreasing frequency of pore emptying according to topologic type in the order: $I1 > I2 > I2A > I3 > I4$ (Figure 7). They also show that the frequency of topologic types in the model is: at S_{ni}, $I3 > I2 > I2A > I1$ and, at S_{nr}, $I3 > I2A > I2 > I1$ (Figure 8).

At S_{ni}, the five different sizes of pores are occupied by mercury with approximately equal frequency but, at S_{nr}, there is greater occupancy by mercury of the larger two sizes of pores than the smaller three sizes of pores (Figure 9).

4. Results of Water-Oil Experiments

The model was saturated with a water-glycerine solution (68 mPa · s) and this was displaced by paraffin oil (46 mPa · s) to an oil saturation (S_{ni}) of ~80–90%. There is a smaller frequency of topologic types $I4$ and $I3$ in the water-oil system than in the air-mercury system at a drainage saturation of ~85%. This difference between the incompressible and compressible wp cases indicates that wp cannot communicate perfectly through thin films. Water advanced during imbibition at a mean velocity of $\sim 1.5 \times 10^{-5}$ m per second which is equivalent to a capillary number (N_{ca}) of approximately 10^{-4}. Displacement was of the frontal drive type with no cluster growth observed. Fluid saturations at the beginning ($S_{ni} = 100 - S_{wi}$) and end (S_{nr}) of imbibition are given in Table I.

A record was made of the fluid topology of pores from which oil withdrew during imbibition (Figure 10) and of the fluid topology (Figure 11) and sizes

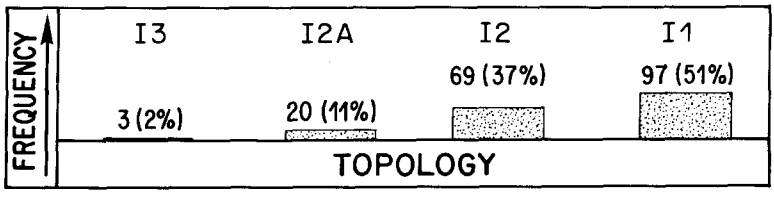

Fig. 10. Fluid topology of pores in which water displaced oil during imbibition from an initial condition with 85% of pores occupied by oil. Percentages are with respect to the total number of pores from which oil was observed being displaced by water.

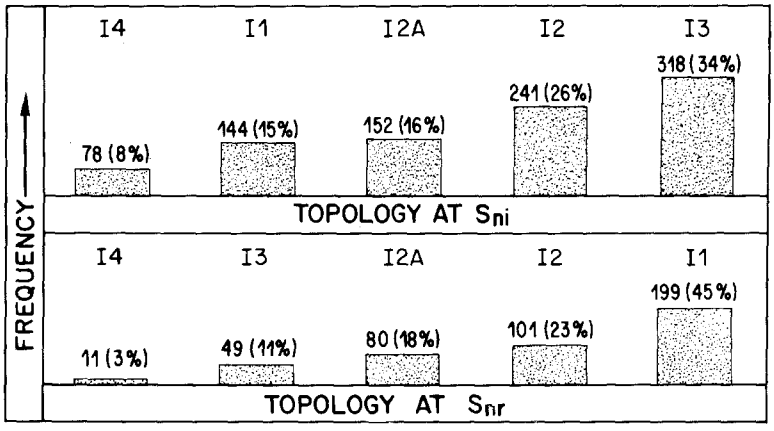

Fig. 11. Fluid topology for pores occupied by nwp at $S_{ni} = 85\%$ and $S_{nr} = 40\%$, for UPT model.

(Figure 12) of pores occupied by nwp at S_{ni} and S_{nr} for comparison with the result from the air-mercury system.

5. Discussion

5.1. EFFECTS OF FLUID TOPOLOGY DURING IMBIBITION

The capillary pressure at which nwp withdraws from a pore during imbibition is a function of the size and shape of the pore and also of the size, shape, position, and nwp occupancy of directly connected throats.

Figure 13A illustrates a pore of diameter X_P with four throats of equal width X_T symmetrically placed. The depth of the pore (Y_P) and of the throat (Y_T), perpendicular to the page, are taken to be equal ($Y_P = Y_T = Y$). An $I2$ interface of diameter X_I is illustrated for a zero contact angle condition at the position where it intersects the pore wall (break-off). The relationship between X_P, X_T, and X_I is given by

$$X_P = 2\left|\left|\left(\frac{X_T - X_I}{2}\right) + (X_I X_T - X_T^2)^{1/2}\right|^2 + \frac{X_T^2}{4}\right|^{1/2} \tag{4}$$

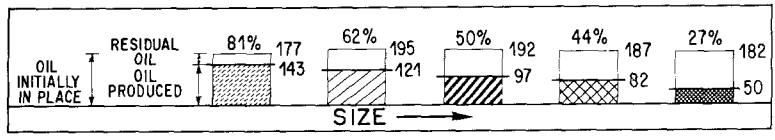

Fig. 12. Illustrates the amount of nwp (oil) initially in place (S_{ni}), oil residual (S_{nr}) and oil produced during imbibition ($S_{ni} - S_{nr}$) for pores of five different sizes. Above each column, oil produced is shown as a percentage of oil initially in place. Same system as for Figures 10 and 11.

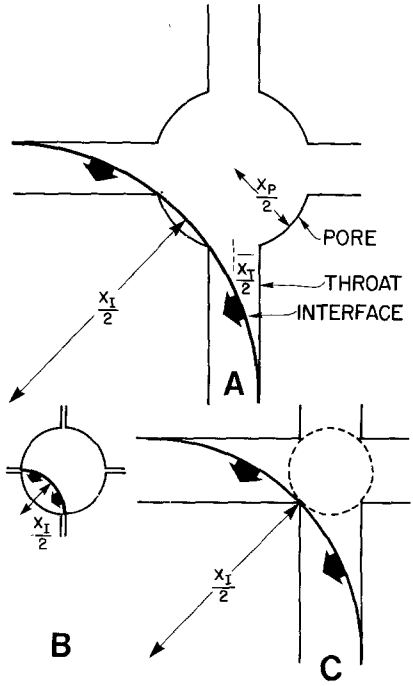

Fig. 13. Interfaces at positions of break-off in pores which have pore to throat diameter ratios which are intermediate (A), maximum (B), and minimum (C).

$I2$ interface positions for break-off with small throats and with large throats are shown in Figures 13B and 13C, respectively. For very small throats, X_I approaches X_P and the capillary pressure for $I1$ and $I2$ events are equal.

Figure 14 illustrates how the ratio of capillary pressures for $I2$ and $I1$ events (P_{I2}/P_{I1}) is related to aspect ratio (X_P/X_T) and to Y/X_T. As can be seen from Figures 13B and C, with decreasing throat diameter in relation to pore diameter, P_{I2} approaches P_{I1}. The ratios of dimensions for pores and throats in the model used for this study (Figure 3) are indicated on the diagram.

In Figure 14 it was assumed that $Y_P = Y_T = Y$ and this is approximately the condition in the model studied. However, where $Y_P \neq Y_T$, use Y_T/X_T as Y/X_T and to calculate P_{I1} use Y_P as Y. Where adjacent throats are not of equal width ($X_{T1} \neq X_{T2}$), use $X_T = (X_{T1} + X_{T2})/2$ and where depth $Y_{T1} \neq Y_{T2}$, use $Y_T = Y_{T1} + Y_{T2}/2$. Equations (1), (2), and (4) can be applied and Figure 14 modified for the case of interest.

Figure 15 shows the effective diameter D (Equation (2)) of pores normalised with respect to the effective diameter of the smallest pore (size 1) versus capillary pressure (P) normalised with respect to P_{I1} for the smallest pore (size 1). The left portion of the diagram (A) shows that interfaces with $I1$ topology will all withdraw from pores at higher capillary pressures than is required for withdrawal

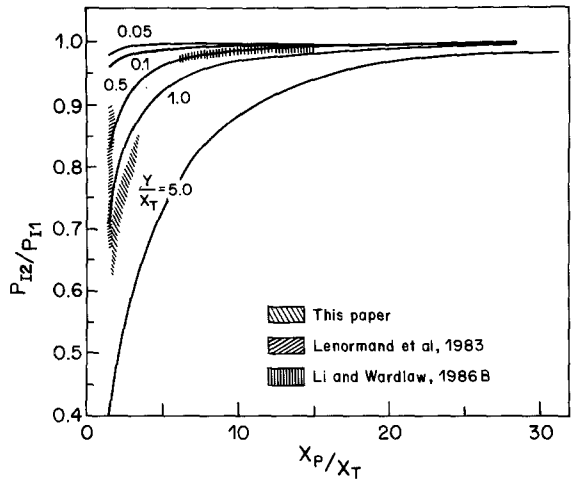

Fig. 14. Pore to throat aspect ratio (X_P/X_T) versus ratio of capillary pressures for $I2$ and $I1$ events (P_{I2}/P_{I1}) and several ratios of Y/X_T. Pores and throats have the same depth ($Y_P = Y_T = Y$).

of $I2$ interfaces, *regardless of pore or throat size*, in this model. These analytical results obtained with Equations (1), (2), and (4) are consistent with the experimental findings that fluid topology has more influence on interface movements during imbibition than do the sizes of individual pores. Pores with fluid topology

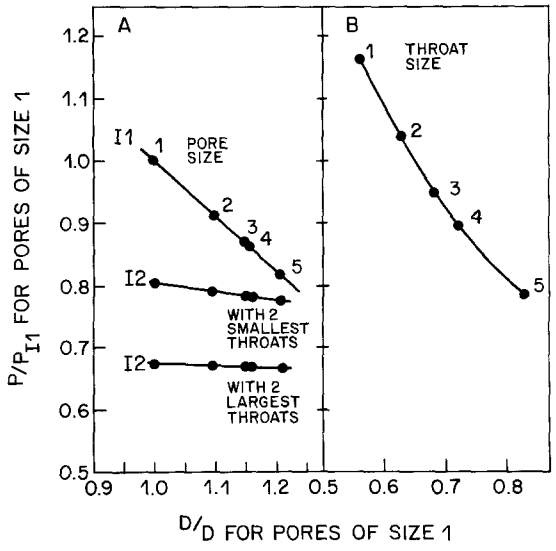

Fig. 15. (A) Effective diameter of pores normalized with respect to pores of size 1 versus capillary pressure (P) normalized with respect to capillary pressure for $I1$ events in pores of size 1. The relative capillary pressures for $I1$ and $I2$ events in pores of five sizes are shown. (B) The relative capillary pressures for snap-off in throat events are shown for pores of size 1 and throats of five different sizes from smallest (1) to largest (5).

$I1$ or $I2$ empty in preference to all other types (Figures 7 and 10) in both the air mercury and water-oil systems. However, pore size has some influence during withdrawal as is shown by the weak relationship for fewer of the larger pores to empty (Figures 9 and 12). This preference is stronger for the water-oil system than for the air-mercury system.

In summary, if the pore-throat aspect ratio is small and if the range of sizes of pores is relatively small, as in the model considered here (Figure 14), P_{I2} is much lower than P_{I1}, and fluid topology provides the primary control on interface movements. Alternatively, if the pore-throat aspect ratio is large and if the range of the sizes of pores is relatively large P_{I2} is close to P_{I1}, and pore size will provide the primary control on interface movements.

The significance of this difference is that the displacement efficiency is much higher where fluid topology exerts the major control. Withdrawal in the topologic sequence ($I1 > I2 > I2A > I3 > I4$) favours nwp to withdraw first from 'dead end' branches, in the continuous nwp network, without breaking the continuity of the nwp conducting pathways to the nwp sink.

This can be demonstrated using computer models. A computer simulation was performed in a random two-dimensional network of pores and throats with four throats connected to each pore. Nonwetting phase withdrew from pores in a sequence strictly related to pore size. S_{wi} was 28% ($S_{ni} = 72\%$), S_{nr} was 67% and displacement efficiency (nwp displaced as a percentage of nwp in place at S_{wi}) was 7% (Li *et al.*, 1986).

In a similar model, pores with $I1$ topology were emptied from an area of 20×40 pores until no further $I1$ types were present. At S_{ni}, 74% of pores were occupied by nwp and, after removal of all $I1$ types, 52% of pores remained occupied by nwp. This is a displacement efficiency of 30% and S_{nr} had not yet been reached, which provides further evidence that displacement efficiency is greater where withdrawal occurs by fluid topology sequence rather than according to pore size.

5.2. RELATIONSHIPS OF FLUID TOPOLOGY TO SATURATION

In the preceding we have shown the importance of fluid topology to the sequence and efficiency of pore emptying during imbibition. We now note that the frequency of fluid topologic types changes systematically during drainage and imbibition. Increasing nwp saturation during drainage increases the frequency of the more highly connected nwp fluid topologies ($I3$ and $I4$) and, in the case of compressible wp and 100% nwp saturation, 100% of pores are of type $I4$. Conversely, decreasing nwp saturation during imbibition eventually increases the less highly connected nwp topologies ($I2$ and $I1$).

Figure 16 illustrates data points obtained for the air-mercury system in the UPT model and approximate extrapolations illustrating frequency curves for fluid topology as a function of nwp saturation (S_n). The frequencies were obtained for areas with ~1200 pores. The initial nwp occupancy of pores is ~74% at

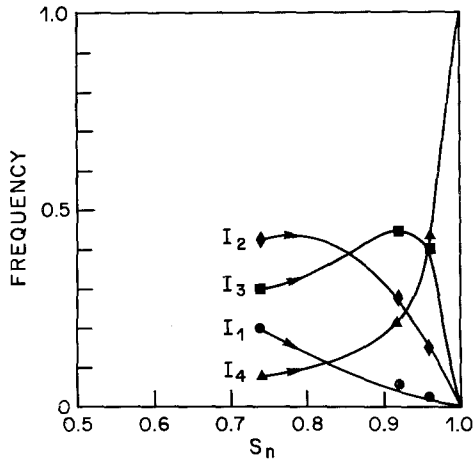

Fig. 16. The frequency of pores having *I*1, *I*2, *I*3 and *I*4 topology are shown as a function of nwp saturation (S_n) for the air-mercury system during drainage.

breakthrough which is higher than the site percolation threshold of 59% for a square lattice (Stauffer, 1985, p. 17). The relatively high value in the experiment is related to the small size of the network and the relatively large pressure increments which caused overstepping of the minimum pressure for breakthrough.

The frequency with which pores with a particular topology emptied during imbibition was observed to be the same for air-mercury (Figure 7) as for water-oil (Figure 10) systems ($I1 > I2 > I2A > I3 > I4$). Although *I*1 and *I*2 types empty more frequently, they are not necessarily reduced in frequency in the remaining population of topologic types during nwp withdrawal. As illustrated in Figure 17,

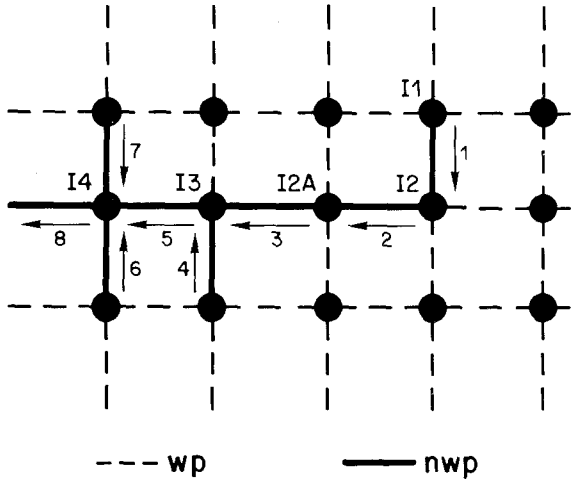

Fig. 17. Withdrawal of nwp from pores with *I*1 topology causes nwp to empty from pores which previously had *I*2, *I*2A, *I*3 and *I*4 topology. The arrows with adjacent numbers show the order of withdrawal events.

withdrawal of nwp from pores with $I1$ topology can cause nwp to withdraw from pores which previously had $I2$, $I2A$, $I3$ and $I4$ topology. Thus, the fluid topology of a given pore can change during imbibition. It can be expected that the frequency of topologic types changes continuously during imbibition, as a function of saturation, in a manner which eventually favours an order $I1 > I2 > I3 > I4$. This order was observed at S_{nr} for the water-oil system initiated at $S_{ni} = 85\%$ and for the air-mercury system initiated at $S_{ni} = 95\%$.

5.3. SNAP-OFF IN THROATS

Figure 15B illustrates the normalized capillary pressures at which snap-off could be expected in throats using the results of Li and Wardlaw (1986a) for the air-mercury system with an air advancing contact angle of 45°. Snap-off in throats of sizes 1 and 2 would be expected at higher capillary pressures than $I1$ or $I2$ events in pores of size 1 (Figure 15A). In fact, few such events were observed in the experiments reported here, because of inadequate wp supply along surfaces to potential snap-off sites. Snap-off may be relatively uncommon in both unconsolidated sands and consolidated rocks, especially where imbibition commences at high nwp saturation and for floods performed at high capillary number.

5.4. APPLICATION OF FINDINGS

The finding that the efficiency of nwp displacement is greater if interface motions occur according to fluid topology sequence rather than to pore size order may provide an explanation for the high displacement efficiency observed in unconsolidated sands and in bead packs. In a disordered packing of glass spheres, Morrow (1970) and Morrow *et al.* (1981) found that, for a water-wet, water-oil system, S_{ni} was ~92% and S_{nr} ~ 15% of pore volume giving a displacement efficiency of ~84%. This large displacement efficiency is incompatible with withdrawal from pores in a sequence related to size.

Computer simulation of a three-dimensional model with $z = 6$ and random arrangement of pores and throats had $S_{wi} = 21\%$ ($S_{ni} = 79\%$), $S_{nr} = 69\%$ and displacement efficiency of 12.6% (Li *et al.*, 1986). Nonwetting phase was withdrawn from pores in a sequence strictly related to pore size and clearly is much less efficient than the 84% obtained experimentally in bead packs and sand packs. A possible explanation of the high withdrawal efficiency obtained for sand packs is that fluid topology exerts a major control on withdrawal sequence.

A further application of the results is in interpreting the structure of a porous medium from capillary pressure curves (Li *et al.*, 1986). The 'rules' which govern interface motions during imbibition are more complex if it is necessary to recognize fluid topology as well as the sizes of pores and throats occupied by nwp. These 'rules' must be known in order to predict the displacement of one immiscible fluid by another in a porous medium and to interpret pore-throat structure from capillary pressure curves.

6. Conclusions

(1) Displacement of nwp by wp (imbibition) may occur by frontal drive, by cluster growth or by a combination of these processes. Wetting phase flow in surface roughness or along the edges and corners of pores is a requirement for cluster growth and is possible only where capillary forces are large in relation to viscous forces. Experiments show that, in addition to low capillary number, lower nwp saturations at the start of imbibition favour cluster growth.

(2) Fluid topology can have more influence on interface movements during imbibition than during drainage. The advancing front is much more regular and the displacement efficiency higher where fluid topology exerts the major control on interface movements. Displacement efficiency is higher because nwp first withdraws from 'dead end' branches in the continuous nwp network, without breaking the continuity of nwp conducting pathways. High initial nwp saturation, small variability of pore size and small pore to throat size diameter ratio all are factors which increase the effects of fluid topology in determining nwp withdrawal sequence. Fluid topology changes systematically as a function of nwp saturation during drainage and imbibition.

(3) The influence of fluid topology may contribute to high displacement efficiency during nwp displacement in unconsolidated sands.

Acknowledgements

The authors thank Mr W. Wright and Mr D. Forbes for assistance in conducting experiments and analysing data. We also thank Dr W. G. Laidlaw, Department of Chemistry, for discussions and assistance with some of the computations. Funds for this project were provided by the Alberta Oil Sands Technology Research Authority and are gratefully acknowledged.

References

Chatzis, I. and Dullien, F. A. L., 1981, Mercury porosimetry curves of sandstones. Mechanisms of mercury penetration and withdrawal, *Powder Technol.* **29**, 117–125.

Chen, J. D., 1986, Some mechanisms of immiscible fluid displacement in small networks, *J. Colloid Interface Sci.* **110–2**, 488–503.

Dullien, F. A. L., Lai, F. S. Y., and MacDonald, I. F., 1986, Hydraulic continuity of residual wetting phase in porous media, *J. Colloid Interface Sci.* **109–1**, 201–218.

Lenormand, R., Zarcone, C., and Sarr, A., 1983, Mechanisms of the displacement of one fluid by another in a network of capillary ducts, *J. Fluid Mech.* **135**, 337–353.

Lenormand, R. and Zarcone, C., 1984a, Role of roughness and edges during imbibition in square capillaries, SPE of AIME, Annual Meeting, Houston, Texas, pp. 1–17.

Lenormand, R. and Zarcone, C., 1984b, Growth of clusters during imbibition in a network of capillaries, in F. Family and D. P. Landau (eds.), *Kinetics of Aggregation and Gelation*, Elsevier, Amsterdam 1984, pp. 177–180.

Li, Y. and Wardlaw, N. C., 1986a, The influence of wettability and critical pore-throat size ratio on snap-off, *J. Colloid Interface Sci.* **109–2**, 461–472.

Li, Y. and Wardlaw, N. C., 1986b, Mechanisms of nonwetting phase trapping during imbibition at slow rates, *J. Colloid Interface Sci.* **109–2**, 473–486.

Li, Y., Laidlaw, W. G., and Wardlaw, N. C., 1986, Sensitivity of drainage and imbibition to pore structures as revealed by computer simulation of displacement process, *Advances in Colloid and Interface Sciences* **26**, 1–68.

Mahers, E. G. and Dawe, R. A., 1985, Visualisation of microscopic displacement processes within porous media in EOR-capillary pressure effects, in 3rd European Meeting on Improved Oil Recovery, Rome, April 1985, pp. 1–10.

Mason, G. and Morrow, N. R., 1984, Coexistence of menisci and the influence of neighbouring pores on capillary displacement curvatures in sphere packings, *J. Colloid Interface Sci.* **100–2,** 519–535.

McKellar, M. and Wardlaw, N. C., 1982, A method of making two-dimensional glass micromodels of pore systems, *J. Can. Petrol. Technol.* **21–4**, 39–41.

Mohanty, K. K., Davis, H. T., and Scriven, L. E., 1980, Physics of oil entrapment in water-wet rock, SPE of AIME, Annual Meeting, Dallas, Texas, pp. 1–16.

Mohanty, K. K., Davis, H. T., and Scriven, L. E., Thin films and fluid distributions in porous media, in D. O. Shah (ed.), *Surface Phenomena in Enhanced Oil Recovery*, Plenum, 1981, pp. 595–609.

Mohanty, K. K. and Salter, S. J., 1982, Multiphase flow in porous media: II, Pore-level modelling, SPE of AIME, Annual Meeting, New Orleans, LA, pp. 1–22.

Morrow, N. R., 1970, Irreducible wetting-phase saturations in porous media, *Chem. Eng. Science* **25**, 1799–1815.

Morrow, N. R., 1971, The retention of connate water in hydrocarbon reservoirs. *J. Can. Petrol. Technol.* **10**, 47–55.

Morrow, N. R., Chatzis, I., and Crocker, M. E., 1981, Measurement and correlation of conditions for entrapment and mobilization of residual oil, Department of Energy, BETC/3251–12.

Stauffer, D., 1985, *Introduction to Percolation Theory*, Taylor and Francis, London, p. 17.

Takamura, K., 1982, Microscopic structure of Athabasca oil sand, *Can. J. Chem. Eng.* **60**, 538–545.